Nonequilibrium electron tunneling in metal-insulator-metal junctions*

J. G. Adler, H. J. Kreuzer, and J. Straus
Department of Physics, University of Alberta, Edmonton, Alberta, Canada
(Received 23 July 1974)

The small structure in the conductance curve near zero bias of metal-insulator-metal tunnel junctions has been studied extensively. These experiments are analyzed in detail in a nonequilibrium model. It is shown that this type of zero-bias anomaly can be accounted for entirely by an electron bottleneck arising from the blocking of tunneling states due to nonzero electron relaxation times.

I. INTRODUCTION

Electron tunneling in normal metal-insulator-metal (M-I-M) junctions has revealed a wealth of information on the tunneling process itself and on microscopic excitation mechanisms in the metals and oxide barrier.[1,2] Since many of the effects observed in the current-voltage characteristics of junctions are small one usually studies the dynamic conductance $\sigma(V) = dI/dV$ as well as its derivative $d\sigma/dV$. Examining the gross features of a tunneling-conductance curve as shown in Fig. 1 one notes a more or less parabolic shape for biases up to several hundred millivolts.[3] A closer scrutiny in the region near zero bias, however, reveals a sharp conductance dip of the order of a few percent of the zero-bias conductance σ_0 as shown in the insert in Fig. 1. Such conductance dips are usually referred to as zero-bias anomalies (ZBA). In order to compare different junctions without loss in generality our curves have been normalized by the zero-bias conductance σ_0 as shown in Fig. 1. As we will show later, junction asymmetry and counter-electrode effects do not concern us in this paper; therefore we will present in many instances the even part of the conductance and its derivative. The odd part is usually small and linear as shown in Fig. 2. A typical plot of $(1/\sigma_0)(d\sigma_e/dV)$ is given in Fig. 3 for a Pb-Pb junction.[4] The peaks in the region above ~ 20 meV arise typically from inelastic barrier excitations[5] (oxide phonons, impurity excitations, etc.). The structure in the 2- to 20-meV region has been identified as metal-phonon[6] excitations. These effects can be understood on the microscopic level as inelastic electron tunneling through opening up of new channels at and above the excitation energies. In this paper we shall concern ourselves only with the additional structure around a few meV. This structure is visible below 10 K and grows rapidly as temperature decreases in contrast to the temperature-independent inelastic-excitation-assisted tunneling.

A number of different mechanisms have been proposed for certain types of ZBA and checked experimentally. We briefly want to review the major mechanisms in order to define the effect we are looking at.

Zeller and Giaever[7] have shown that large zero-bias conductivity dips can be achieved if tunneling occurs through intermediate states on metal particles embedded in the oxide barrier. Typical results of their ZBA are (i) linear decrease of σ_0 with increasing temperature; (ii) no magnetic field dependence; (iii) increase of ZBA with decreasing particle size. It is to be expected that the Zeller-Giaever mechanism is only important in junctions specifically fabricated for this kind of a ZBA.

A large ZBA similar to the Al-Ni junction shown in Fig. 1 arises if magnetic impurities are present in the oxide barrier.[1,8] In this paper we shall not be dealing with either this or the Zeller-Giaever anomalies.

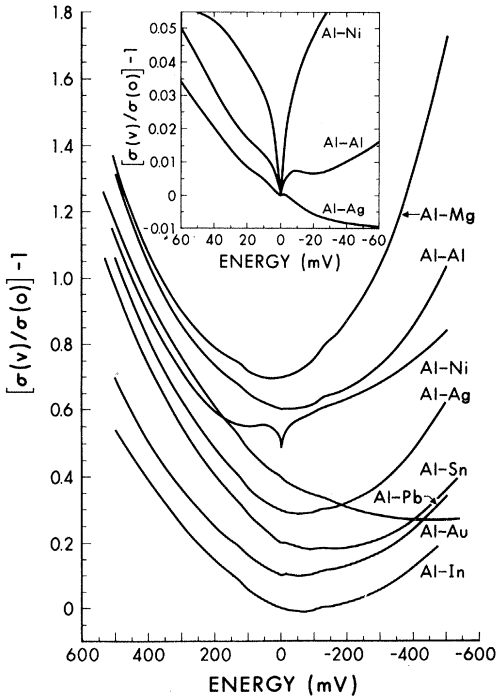

FIG. 1. Typical behavior of tunnel conductance for various junctions. The insert illustrates the behavior in the zero-bias region.

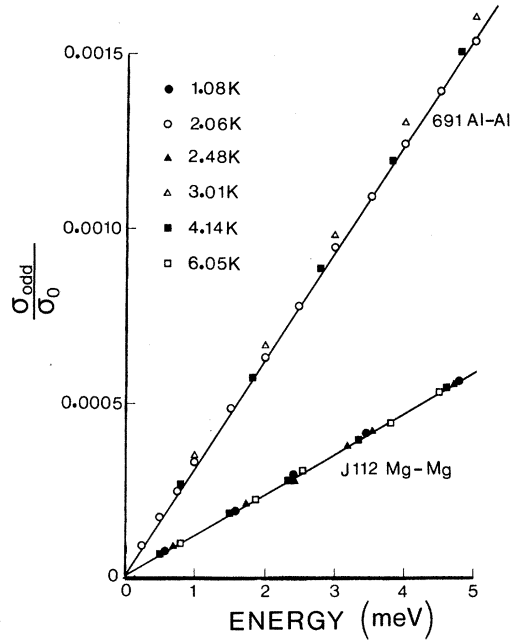

FIG. 2. Normalized odd conductance in the zero-bias region.

Junctions without metal particles or magnetic impurities built into the barrier show a much weaker ZBA involving a decrease of only a fraction of 1% in conductance near zero bias and are usually restricted to a voltage range less than 5 mV. We have observed such small ZBA in a variety of junctions (Al-Al, Al-Pb, Pb-Pb, Mg-Au, Mg-Mg, etc.). If one or both metals are superconducting any possibility of mistaking the onset of superconductivity for a ZBA can be clearly eliminated as shown in

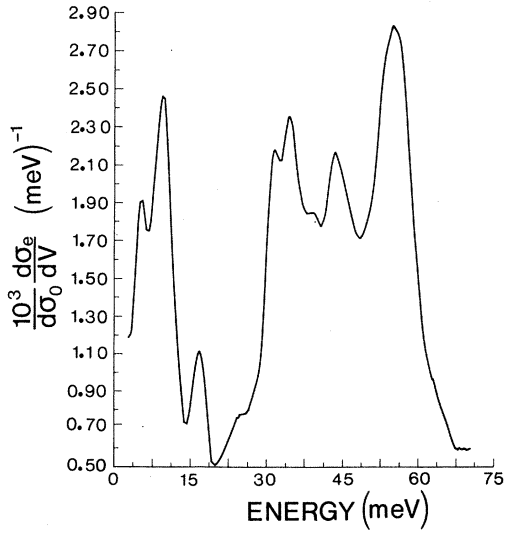

FIG. 3. Normalized even derivative of conductance for Pb-O-Pb junction. The region below 3 meV which induced the ZBA peak is deleted for clarity.

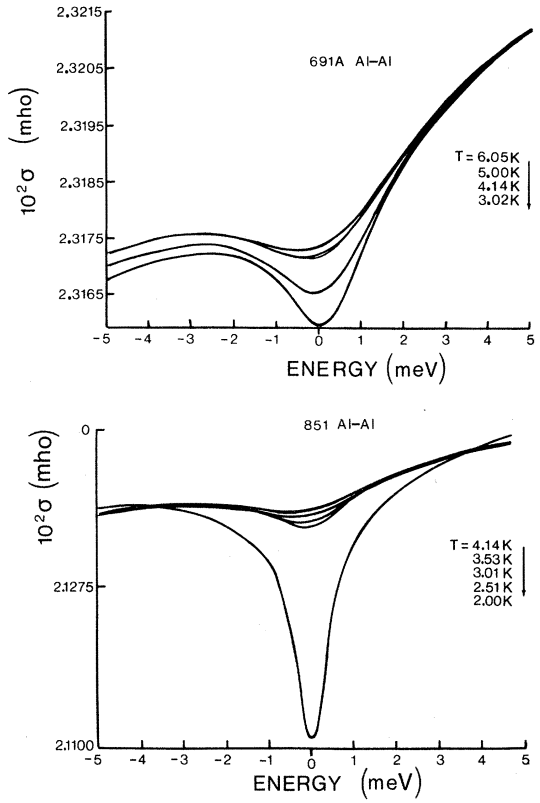

FIG. 4. Temperature dependence of conductivity of Al-Al junctions demonstrating the drastic effect of superconductivity at 2 K.

Fig. 4. We note that this 680-Å Al film with an elevated transition temperature of 2 K shows superconductivity quite clearly. The small ZBA which we deal with is a universal feature of M-I-M junctions in the normal state and is also demonstrated in Fig. 5 where both metals are clearly normal. Both the junctions of Figs. 4 and 5 show the same temperature[9] and magnetic field dependence[10] which clearly excludes attributing these ZBA to any residual superconductivity effects.[11]

It will be shown in this paper that the small ZBA are due to the nonequilibrium aspect of the electron transport in tunneling which results in blocking of tunneling states due to nonzero electron relaxation times most important just above the Fermi surface.[9] The resulting electron bottleneck shows up as a dip in the tunneling conductivity in all junctions unless more effective blocking mechanisms are present.

The theoretical model to be advanced in Sec. II predicts the temperature dependence and allows discussion of various size effects. Moreover we will be able to estimate impurity scattering times and the electron-phonon relaxation time. The detailed predictions of the model have been verified by numerous experiments to be discussed in Sec.

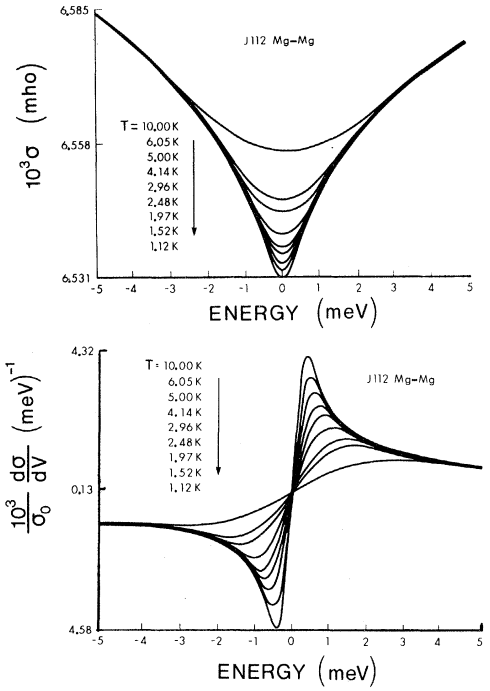

FIG. 5. Zero-bias anomaly of a typical Mg-Mg junction for various temperatures.

III. A discussion of the magnetic field dependence has been given elsewhere.[10]

II. THEORETICAL MODEL

To understand the nonequilibrium aspect of electron tunneling let us follow the history of an electron in a semiclassical picture neglecting many-body effects. Consider for simplicity a junction consisting of an infinite metal on the left side and a metal film of thickness L on the right side. Call the tunneling direction the z axis and assume infinite extension of the junction in the x, y plane. An electron starting on the left will tunnel to the right at a rate $v_z P(v_z)/2L = 1/\tau_B$, where $P(v_z)$ is its penetrability through the barrier and $v_z \sim v_F$ is the z component of its velocity. In our classical picture, $2L/v_z$ is the time it takes the electron to travel from the right barrier interface to the back wall of the right metal and return. In a quantum-mechanical picture the size of the metal film would enter in the same way through the density of states in a finite box. In the standard treatments of tunneling it is next assumed that the electron relaxes spontaneously to the Fermi sea thus making its state available to the next tunneling electron. In this quasiequilibrium theory the tunneling current is given by

$$I(V) = \frac{4\pi emA}{h^3}\int_0^\infty dE[f^0(E - eV - \mu_1) - f^0(E - \mu_1)] \times \int_0^E P(E_z)\,dE_z, \tag{2.1}$$

where f^0 is the Fermi-Dirac distribution function and A is the junction area. In a more realistic theory, however, it will take the electron a nonzero time to relax to the Fermi sea, thus blocking an otherwise available tunneling state leading to a decrease in conductance over a voltage range in which electron relaxation times are appreciably different from zero. According to Fig. 6 an electron will occupy its excited state until it is scattered out of the tunneling direction via impurity scattering with a relaxation time τ_i or via electron-phonon scattering $\tau_{ep}(\epsilon, T)$. In τ_i we include all scattering mechanisms that are energy and temperature independent over the range covered by the experiments. In the region of interest, at low temperatures ($T < 10$ K) and low energies ($\leq k\Theta_D$), the temperature- and energy-dependent electron-phonon relaxation time is given by[12]

$$\tau_{ep}(\epsilon_k, T)^{-1} = \frac{2\pi}{\hbar}\sum_{\vec{k}'} |M(\vec{q})|^2[(N_q^0 + 1 - f_{k'}^0) \times \delta(\epsilon_k - \epsilon_{k'} - \hbar\omega_q) + (N_q + f_{k'}^0)\delta(\epsilon_k - \epsilon_{k'} + \hbar\omega_q)]. \tag{2.2}$$

where $\vec{q} = \vec{k} - \vec{k}'$ is the phonon momentum and N_q^0 is the Bose-Einstein distribution function. We can

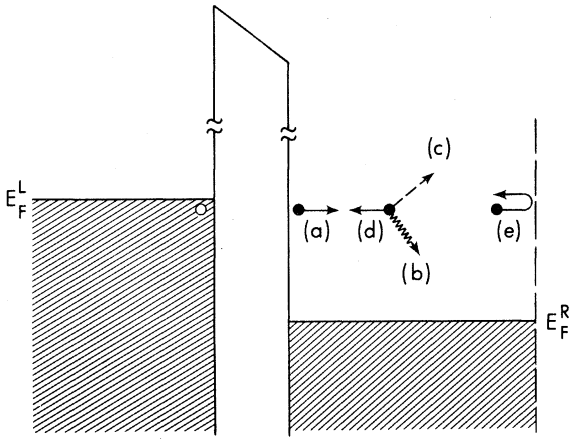

FIG. 6. An electron that tunnels through the barrier will leave a hole in the left electrode and occupy a state (a) in the right electrode. This electron will travel away from the barrier in the right electrode and may be scattered by various processes: (1) Inelastic scattering with emission or absorption of a phonon (b) will alter both the energy and momentum of the electron; this type of process will be described by an energy- and temperature-dependent relaxation time $\tau_{ep}(\epsilon, T)$, where ϵ is the energy measured relative to the chemical potential of the right electrode and T is the temperature. (2) Elastic scattering by impurities, (c) and (d), will alter only the momentum of the electron and will be accounted for by a constant relaxation time τ_i. (3) Boundary scattering, if specular, (e), will reverse the component of the momentum of the electron perpendicular to the barrier.

now write down the balance equations for the nonequilibrium distribution functions $f=f^0+\delta f$ for the left and right metal films:

$$\frac{\partial f_r}{\partial t}=\frac{1}{\tau_B}(f_l-f_r)-\delta f_r\left(\frac{1}{\tau_{e\phi}^r}+\frac{1}{\tau_i^r}\right),$$
$$\frac{\partial f_l}{\partial t}=-\frac{1}{\tau_B}(f_l-f_r)-\delta f_l\left(\frac{1}{\tau_{e\phi}^l}+\frac{1}{\tau_i^l}\right). \quad (2.3)$$

In steady state we get

$$f_l-f_r=(f_l^0-f_r^0)[1-g(\epsilon, T)] \quad (2.4)$$

with the blocking factor

$$g(E, T)=\frac{1/\tau_B}{1/\tau_B+[\tau_l(eV-E, T)+\tau_r(E, T)]^{-1}}, \quad (2.5)$$

where $\tau^{-1}=\tau_{e\phi}^{-1}+\tau_i^{-1}$.

Next we calculate the tunneling current equation (2.1) using these steady-state occupation functions instead of their equilibrium values. For the normalized blocking conductance $\delta\sigma(V)\sigma_0=[\sigma(V)-\sigma_0]/\sigma_0$ we find

$$\frac{\delta\sigma(V, T)}{\sigma_0}=-\int_{-\infty}^{+\infty}d\epsilon\left(-\frac{df^0(\epsilon, T)}{d\epsilon}\right)\left(\frac{\tau_l(\epsilon+eV, T)}{\tau_B^l}+\frac{\tau_r(\epsilon+eV, T)}{\tau_B^r}\right). \quad (2.6)$$

The second derivative is then given by

$$\frac{1}{\sigma_0}\frac{d}{dV}[\sigma_e(V)]=\int_0^{+\infty}\frac{dx}{(1+e^x)(1+e^{-x})}[S(eV-xkT)+S(eV+xkT)] \quad (2.7)$$

with

$$S(\epsilon)=-\frac{d}{d\epsilon}\left(\frac{\tau_l(\epsilon, T)}{\tau_B^l}+\frac{\tau_r(\epsilon, T)}{\tau_B^r}\right). \quad (2.8)$$

Before we proceed to the experimental verification of our model, a short discussion of the general aspects is in order. Let us assume for simplicity that the left-hand metal is in equilibrium $f_l=f_l^0$. This can be achieved, e.g., by making its thickness very large, i.e., $\tau_B^l\to\infty$. Then blocking arises from the right-hand metal only. To be able to evaluate $\tau_{e\phi}(eV, T)$, let us further assume that $\alpha^2(\omega)F(\omega)=a\omega$ is effectively linear in ω in the relevant energy region,[13] then

$$\tau_{e\phi}^{-1}(T)\approx\frac{\pi a}{\hbar}[(eV)^2+(\pi kT)^2], \quad (2.9)$$

and we find at $T=0$ K

$$\frac{\delta\sigma(V)}{\sigma_0}=\frac{1/\tau_B}{1/\tau_B+1/\tau_i+(\pi/\hbar)a(eV)^2} \quad (2.10)$$

and

$$\frac{1}{\sigma_0}\frac{d}{dV}[\sigma(V)]=\frac{1/\tau_B a(eV)}{[1/\tau_B+1/\tau_i+(\pi/\hbar)a(eV)^2]^2}. \quad (2.11)$$

These formulas reproduce the experimental data qualitatively and are sketched in Figs. 7 and 8. To get an order-of-magnitude estimate of the relaxation times involved, observe that the conductance dip at zero bias is typically 10^{-3} to 10^{-2} which is equal to

$$\frac{\delta_\sigma(0)}{\sigma_0}=\frac{\tau_i}{\tau_i+\tau_B}. \quad (2.12)$$

thus $\tau_i\sim(10^{-3}\tau_B)$. With typical impurity times $\tau_i\sim10^{-9}$ sec, we get $\tau_B\sim10^{-6}$–10^{-7} sec. Recalling $1/\tau_B\simeq(v_F/2L)P$, we find for a typical thickness of metal films of a few thousand Angstroms a penetrability corresponding to an oxide thickness of a few molecular layers. We should mention here that our model predicts a dependence of the size of the ZBA on the thickness of the metal films, the effect being smaller for thicker films. This thickness dependence is, however, not as dramatic as the zero-temperature formula equations (2.10)–(2.12) suggest, because, e.g., at $T=1$ K and for $eV=0$, $\tau_{e\phi}^{-1}$ is already of the order of τ_B^{-1}, thus reducing the size dependence sharply. This will be checked out experimentally in Sec. IV. Using $\delta\sigma(V)/\sigma_0$ we can fit $\tau_{e\phi}(eV, 0)$ and thus a in $\alpha^2F=a\omega$ with the help of the width of the conductance dip, or the peak position in $(1/\sigma_0)\times(d/dV)$. It should be noted that the three parameters τ_i, τ_B, and a do not enter Eqs. (2.10) and (2.11) independently but in the combinations τ_i/τ_B and $\Gamma=\hbar/\pi a\tau_i$. It is the latter parameter that determines the temperature dependence. To extract a we thus will have to make an assumption on τ_i and vice versa. A comparison with experimental data is presented in Sec. IV.

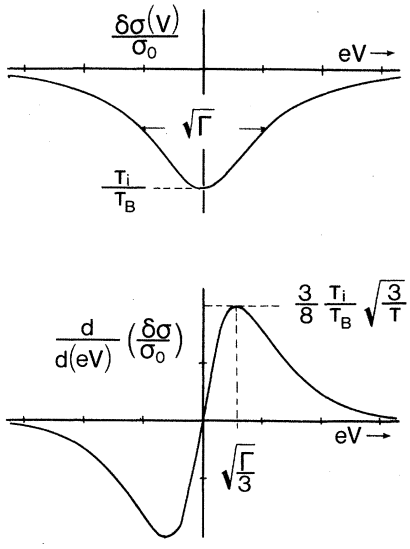

FIG. 7. Calculated, $T=0$ K, behavior of the zero-bias blocking conductance.

III. EXPERIMENTAL TECHNIQUES

In order to compare theory and experiment a large number of junctions were made including the following metals: Al, Ag, Au, Mg, Pb and Pb-Bi alloys. For the purposes of this paper three typical junctions suffice to illustrate all the results. The evaporator used could be operated without ever exposing the junction to air during the entire fabrication procedure. The metals were evaporated at pressures below 10^{-6} Torr. The system used sorption pumping along with an elaborately baffled liquid-nitrogen trap so that contamination (such as hydrocarbons) could be eliminated from the insulating layer. The masking system was such as to allow as many as three junctions to be prepared on the same substrate. These three junctions could share either a common base layer or counterelectrode.

A glow discharge technique of barrier formation was used to prepare tunnel barriers of Mg and Al.[14] The oxidation of Mg in 100 to 200 Torr of pure oxygen with glow discharge current maintained for 1 to 3 min at 5 to 15 mA was sufficient to produce tunnel junctions with resistances around 200 Ω. Aluminum required longer oxidation times (5 to 10 min) and higher pressures (400 Torr) with approximately the same discharge current. The same technique was used to prepare tunnel junctions of Mg in a nitrogen environment. In this case, however, the discharge had to be kept for 40 to 80 min with currents up to 40 mA and pressures between 400 to 600 Torr. The exact composition of this type of barrier is not known and it is a subject of a further investigation. It has been shown[15] that Mg heated in nitrogen environment containing traces of water vapor and oxygen reacts preferably with impurities, forming a compact layer of oxide on the metal, thus inhibiting the formation of the nitride.

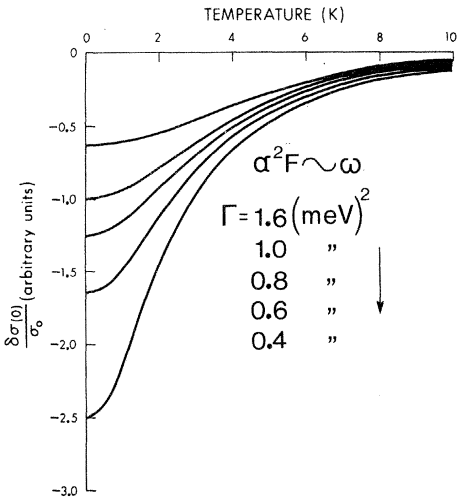

FIG. 8. Blocking conductance at zero bias plotted for various values of Γ described in the text.

In some cases junctions were purposely doped with hydrocarbons[16] during formation of the barrier layer in order to study this effect of this barrier on the ZBA. Junction J112 (Fig. 5) is such a junction and the effect of this doping is discussed in Sec. IV. All other junctions shown in this paper are clean junctions.

The measurements were carried out by a bridge technique similar to that described previously by Adler, Chen, and Straus.[4] In this instance, however, the system was interfaced to a minicomputer[17] showing calibrated second-derivative plots to be obtained at the end of each sweep. This measurement system will be described in a forthcoming paper.

IV. COMPARISON WITH EXPERIMENT

It can be seen from Fig. 1 that a typical tunneling conductance in the region of a few hundred mV can be approximated by an asymmetric parabola of the form

$$\sigma(V) = \sigma_0 + \sigma_1 V + \sigma_2 V^2 + \delta\sigma(V, T), \tag{4.1}$$

where the first three terms describe an ideal temperature-independent (1 to 10 K) background in the absence of ZBA.[18] For a comparison of theory and experiment it is desirable to separate the ZBA from this background. The small asymmetry arising from a temperature-independent linear term shown in Fig. 2 can be eliminated over the energy region of interest if we consider only the even part of the conductance. In particular, if the second-derivative data are available we can write

$$\frac{d\sigma_e}{dV} = 2\sigma_2 V + \frac{d}{dV}[\delta\sigma(V, T)]. \tag{4.2}$$

This enables one to separate the ZBA contribution to the tunnel conductance by simply subtracting a straight line, passing through the origin, with a slope which brings the measured $d\sigma_e/dV$ to zero at about 5 meV. On the other hand if data are available at sufficiently high temperature (say 10 K), then the background can be eliminated by simply subtracting the high-temperature curve. The use of either procedure leads to the same result reducing raw data (Fig. 5) to the pure ZBA contribution (Fig. 9). The equivalence of both methods becomes clear if we examine Figs. 7 and 8 which show the behavior of the ZBA with increasing voltage and temperature.

Typical experimental results for Mg-Mg junctions are shown in Fig. 9. From these data values of V_{max}, the bias at which the maximum (in $1/\sigma_0$) $\times(d/dV)[\delta\sigma_e(V, T)]$) in the even part of the second derivative occurs can be obtained for various temperatures. Figure 10 shows a plot of these ex-

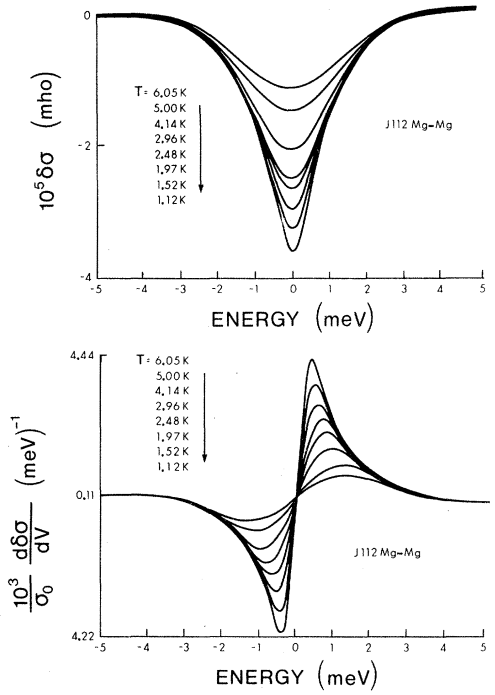

FIG. 9. Reduced data showing the pure blocking effect after subtraction of background from Fig. 5.

perimental data along with theoretical results for values of between 0.4 and 1.2 meV^2. It can be seen that the peak positions are best fitted by Γ

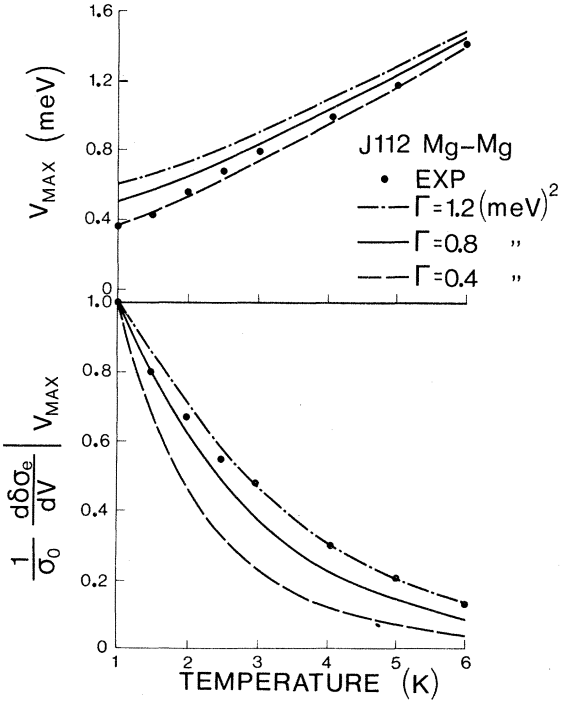

FIG. 10. Peak height and peak position fit for a Mg-Mg junction as discussed in text.

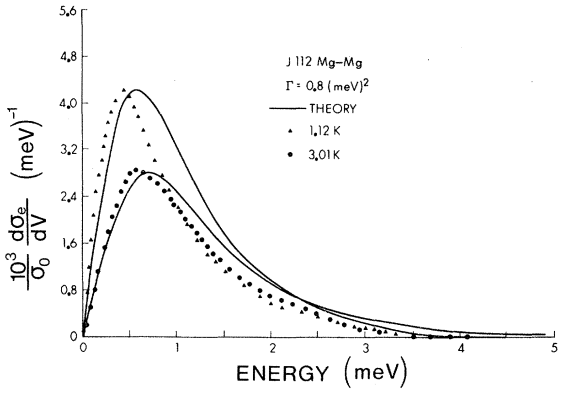

FIG. 11. Fit of even part of the second derivative of the current-voltage characteristics of a Mg-Mg junction compared with theory.

$= 0.4$ meV^2, while the peak heights are best represented by $\Gamma = 1.2$ meV^2. An intermediate value of $\Gamma = 0.8$ meV^2 gives a reasonable fit to the data as shown in Fig. 11. With this choice of Γ the theory then predicts a stronger temperature dependence for the peak amplitudes than experimentally observed. Correspondingly the peak positions are at lower biases than expected. We have observed this small departure from theory in all our junctions and will discuss the reasons for it in Sec. V.

In the absence of any knowledge of the electron-phonon coupling constant for Mg, we have arbitrarily assumed it to be 0.0015 meV^{-1}, which is half that calculated for aluminum.[19] Using this value we obtain

$$\tau_i \approx 2\times10^{-10} \text{ sec} \quad \text{and} \quad \tau_B \approx 1\times10^{-7} \text{ sec}$$

by using $\Gamma = 0.8$ meV^2.

As mentioned in Sec. III the barrier layer of this particular junction has been doped with hydrocarbons. On the other hand for clear junctions one always finds that $\delta\sigma(0)/\sigma_0$ is several times larger, as shown in Fig. 12. The smaller ZBA of the doped junctions is due to increased diffuse scattering at the metal-barrier interface. In clean junctions this interface is sharp, and more specular scattering of electrons in the metals occurs decreasing the amount of deblocking, resulting in a larger ZBA. Replacing the top Mg layer by an Au counterelectrode does not alter the character of the ZBA. This suggests that the deblocking occurs in the stronger coupling metal as expected from the theory. Figure 12 shows the temperature dependence of the conductance of two such junctions. Both of these share a common Au overlayer.

We were also able to study the effect of annealing on these junctions. After measurement, some junctions were allowed to warm up in a vacuum.

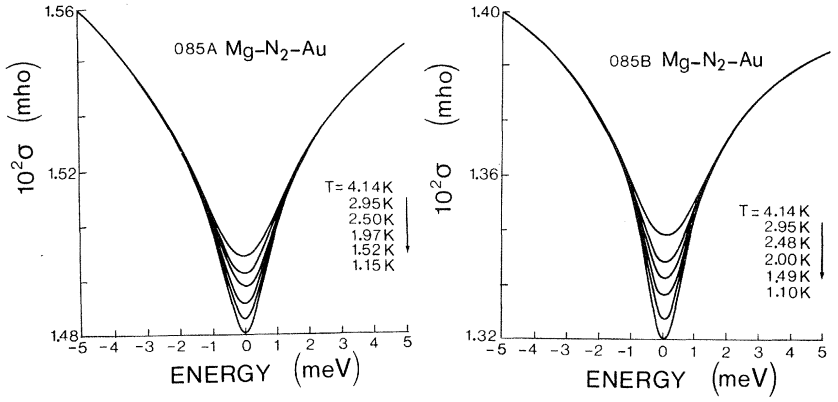

FIG. 12. Tunneling conductance of two Mg-N_2-Au junctions sharing the same gold counterelectrode. The magnesium base layer of junction 85A was 30 000 Å thick, while that of 85B was only 3000 Å thick.

Several days later they were cooled down again and a new set of measurements was made. This annealing increased the resistance of these junctions about $2\frac{1}{2}$ times. The relative magnitude of the conductance dip, characteristic of the zero-bias anomaly, remained unchanged. This shows that the scattering mechanisms which deblock the tunneling electrons are unaltered. In Fig. 13 we show the experimental data for 85B1 (unannealed) and B2 (annealed) together with the fit obtained by adjusting Γ to 0.6 meV^2. The theory again predicts a stronger temperature dependence for the peak amplitudes. As the temperature decreases the peak positions lie below the theoretical curve. The line shapes of $(1/\sigma_0)d\delta\sigma_e/dV$ for $T=1$ K and 3 K are shown in Fig. 14.

As shown in the theoretical part, metals with infinitely thick electrodes are essentially in equilibrium because the density of final states for the incoming electrons is infinite. This assertion was tested with double junctions having a common counterelectrode and base layers of different thicknesses. Also several junctions with thick base layers and counterelectrodes of varying thicknesses were studied and gave the same results. All of these consistently showed smaller zero-bias anomalies in the junctions having the thicker film. Junctions 85A, 85B are representative of these (Fig. 15). We should add that an extensive study of the lateral structure of our junctions has been previously reported in Ref. 20 for the barrier geometry and in Ref. 10 for the film geometry.

V. SUMMARY AND DISCUSSION

In this paper we have concerned ourselves with small low-energy ZBAs in normal M-I-M junctions. We have explained these ZBAs as due to an electron bottleneck arising from nonzero electron relaxation times. We have seen that the temperature dependence is due to electron-phonon relaxation. As has already been shown elsewhere the magnetic field dependence is due entirely to a geometrical size effect.[10]

It should be noted that this theoretical model of nonequilibrium electron tunneling can be generalized to include other kinds of ZBAs as well. For example, the Zeller-Giaever mechanism which produces large ZBAs by trapping electrons on metallic particles embedded in the oxide layer can also be cast in the framework of this theory by setting up the balance equations for a two-step tunneling process with an additional relaxation time for the electrons trapped on the metallic grains.

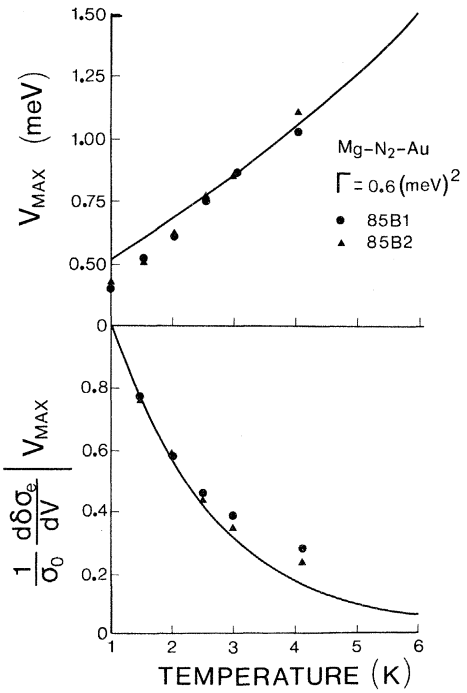

FIG. 13. Fit of peak heights and peak positions for a Mg-N_2-Au junction. The result shows the first run, junction 85B1, along with later results obtained after this junction was allowed to anneal at room temperature, labeled junction 85B2.

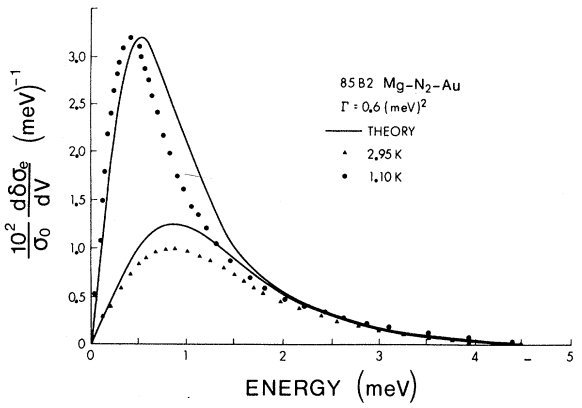

FIG. 14. Typical second derivative for the Mg-N_2-Au junction described in the text.

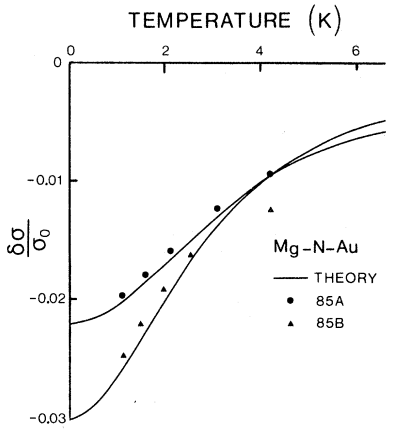

FIG. 15. Zero-bias conductance for the two Mg-N_2-Au junctions described in Fig. 12.

We have neglected one effect in the above theory which becomes important at lower temperatures. This is the presence of nonequilibrium phonons. So far we have only considered the nonequilibrium part of the electron distribution. However, in steady state we also have to account for a nonequilibrium phonon occupation. Assuming that the thermal relaxation of phonons is due to boundary scattering (with a typical time $\tau_{\text{boundary}} \sim 10^{-10}$ sec) which is of the same order as the electron-phonon relaxation time in the ZBA peak region. Thus the number of nonequilibrium phonons δN in steady state will be of the order of the number of nonequilibrium electrons δf. A detailed study[21] of the coupled electron-phonon system shows that the nonequilibrium phonons keep the junction at an effective temperature of about 0.1 to 0.5 K higher than the temperature of the surrounding bath in the ZBA region. Thus at very low temperatures the electron-phonon relaxation will be faster than expected without the nonequilibrium phonons. One of the observable effects will be that the position of the ZBA peak in the derivative of the tunneling conductance will be at a somewhat lower bias than expected from the simpler theory presented in this paper (Figs. 11 and 14).

Finally we want to comment briefly on the influence of nonequilibrium effects on superconducting tunneling. Again we must expect a quasiparticle bottleneck just above the gap. In this case the elastic scattering times become infinite at the gap edge,[22] i.e., at $T=0$ K,

$$\tau_s = \frac{|\epsilon|}{(\epsilon^2 - \Delta^2)^{1/2}} \tau_N ,$$

where τ_s and τ_N are the relaxation times in the superconducting and normal state, respectively. We thus expect total blocking just above the gap edge. For the case of a junction with two identical superconductors this leads to a continuous increase in the tunnel current just above twice the gap energy instead of the discontinuous jump predicted by quasiequilibrium theories. It should be pointed out that the observed discrepancy between theory and experiment has been explained in various ways as arising from strain in the metal films, local heating, gap anisotropies, etc. A detailed investigation of our proposed explanation will be presented elsewhere.

*Work supported in part by the National Research Council of Canada.

[1]C. B. Duke, in *Solid State Physics*, edited by F. Seitz, D. Turnbull and H. Ehrenreich (Academic, New York, 1969), Suppl. 10.

[2]E. L. Wolf, in *Solid State Physics*, (Academic, New York, to be published).

[3]T. T. Chen and J. G. Adler, Solid State Commun. 8, 1965 (1970).

[4]J. G. Adler, T. T. Chen, and J. Straus, Rev. Sci. Instrum. 42, 362 (1971).

[5]J. Lambe and R. C. Jaklevic, Phys. Rev. 165, 821 (1968).

[6]J. M. Rowell, W. L. McMillan, and W. L. Feldmann, Phys. Rev. 180, 658 (1969).

[7]H. R. Zeller and I. Giaever, Phys. Rev. 181, 789 (1969).

[8]J. M. Rowell, J. Appl. Phys. 40, 1211 (1969).

[9]P. N. Trofimenkoff, H. J. Kreuzer, W. J. Wattamaniuk, and J. G. Adler, Phys. Rev. Lett. 29, 597 (1972); in *Proceedings of the 13th International Conference on Low Temperature Physics, Boulder, Colorado*, 1972, edited by W. J. O'Sullivan, K. D. Timmerhaus, and E. F. Hammel (Plenum, New York, 1974) see also W. J. Wattamaniuk, Ph.D. thesis (University of Alberta, 1973) (unpublished).

[10]J. G. Adler, H. J. Kreuzer, and J. Straus, Solid State Commun. 13, 939 (1973).

[11]M. Strongin, A. Paskin, O. F. Kammerer, and M. Garber, Phys. Rev. Lett. 14, 362 (1965).

[12]See, e.g., J. W. Wilkins, *Observable Many Body Effects in Metals* (Nordita, Copenhagen, 1968).
[13]P. B. Allen and R. Silberglitt, Phys. Rev. B 9, 4733 (1974).
[14]J. L. Miles and P. H. Smith, J. Appl. Phys. 34, 2109 (1963).
[15]B. Dupré and R. Streiff, J. Nucl. Mater. 42, 241 (1972).
[16]H. C. Dope (private commication).
[17]J. G. Adler and J. Straus (Rev. Sci. Instr. 46, 158 (1975).
[18]W. H. Brinkman, R. C. Dynes, and J. M. Rowell, J. Appl. Phys. 41, 1915 (1970).
[19]J. P. Carbotte and R. C. Dynes, Phys. Rev. 172, 476 (1968).
[20]J. G. Adler and H. J. Kreuzer, Can. J. Phys. 50, 2842 (1972).
[21]H. J. Kreuzer (unpublished).
[22]J. Bardeen, G. Rickayzen, and L. Tewordt, Phys. Rev. 113, 982 (1959).